3rd CEAS Air&Space Conference
21st AIDAA Congress

Large Attitude Maneuvers of a Spacecraft with Flexible Solar Panels

E. Paolini, F. Curti and M. Parisse
School of Aerospace Engineering, University of Rome La Sapienza, Italy

M. Battilana
CGS S.p.A., an OHB Technology Company, Milan, Italy

Keywords: *attitude, control, flexibility, thrusters, reaction wheels.*

Abstract

This paper faces with the problem of the attitude maneuver control of a spacecraft with large solar panels, actuated by thrusters and reaction wheels. A functional separation has been performed: thrusters are used for attitude maneuvers with a feed forward approach, while reaction wheels are used in closed loop to refine the maneuver. Thrusters allocation is optimized to increase the resulting torque in order to reduce the fuel consumption for the maneuvers. Since the attitude dynamics is influenced by the vibrations due to the flexibility of the solar panels, this effect is taken into account: the attitude dynamics equations are derived using a Lagrangian approach to include the flexibility of the arrays. An optimal control has been implemented in order to reduce fuel consumption while maneuvering the satellite. Numerical simulations have been run to evaluate the AOCS performance, during the large attitude maneuvers, and the pointing accuracy. Results are presented.

1 Introduction

Nowadays many satellites require the ability to perform large angle maneuvers in a fixed time, or in some cases even in minimum time. The problem is often approached trying to simplify the spacecraft dynamics. Therefore deep studies on the rigid body control have been developed for large angle maneuvers [1,2]. Minor efforts have been focused on the control of rigid bodies with flexible appendages. However the problem became of large interest in the mid 90s. Moreover, three axes maneuvers are usually performed by means of a sequence of single-axis rotations. Such maneuvers may take a relatively long time, and their duration can be reduced considerably by performing simultaneous three axes slews. This work deals with the three-axes slew of a spacecraft with flexible appendages. This problem is not only infinite dimensional for the arrays flexibility, but also highly non-linear. Works facing with these problems are for example [3,4,5]. However, the problem can be simplified, considering a discrete parameters model.

The objective of the spacecraft under analysis is the observation of deep space for astronomy purposes from a LEO orbit.
A layout of the spacecraft with its body reference frame, centred in the satellite centre

of mass (CoM), is depicted in Fig. 1. The line of sight of the instruments in the payload module is along X_{sat}; the panels deploy along Y_{sat}. The sun direction shall be kept always in the $-X_{sat}$, Z_{sat} plane. The panels can rotate around Y_{sat} to improve the angle of incidence of the sun rays. Each panel is 1.2 m wide and 5 m long. Table 1 shows the spacecraft dimensions and the estimated moments of inertia: the body frame depicted in Fig. 1 is supposed to coincide with the principal axes reference frame, thus inertia matrix is diagonal. The position of the centre of mass is supposed to lie along X_{sat}; its position varies from 1266.6 mm from the -X_{sat} face at BOL to 1353.5 mm at EOL, ensuring the CoM to lie always within the platform module.

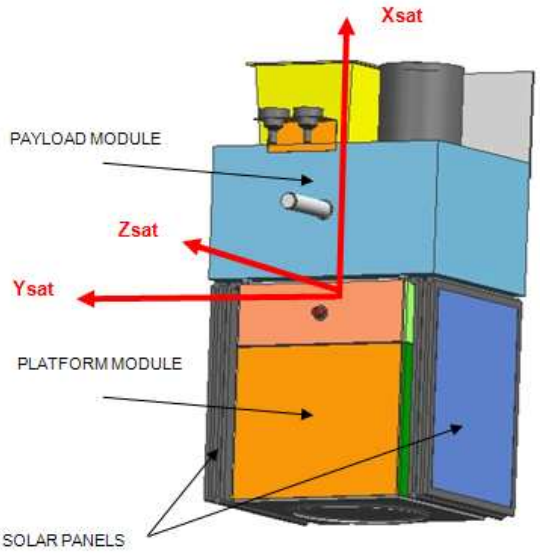

Fig. 1 Spacecraft layout and body frame definition.

Table 1 Spacecraft dimensions and moments of inertia.

PLATFORM X LENGTH [mm]	1445
PLATFORM Y LENGTH [mm]	1240
PLATFORM Z LENGTH [mm]	1240
PAYLOAD X LENGTH [mm]	1505
PAYLOAD Y LENGTH [mm]	1650
PAYLOAD Z LENGTH [mm]	1274
XX INERTIA [kgm^2]	400
YY INERTIA [kgm^2]	1000
ZZ INERTIA [kgm^2]	1200
SOLAR PANEL MASS [kg]	30

The axis of the line of sight of all instruments in the payload module (X_{sat}) shall be rotated for astronomical observations. Considering the maximum field of view of the instruments, the amplitude of the maneuver is $\pm 45°$ around Y_{sat} and Z_{sat}. In addition, the attitude control shall keep the sun direction always in the $-X_{sat}$, Z_{sat} plane; thus a third rotation, around X_{sat}, is required for re-pointing the sun vector in the desired direction. The amplitude of this rotation is calculated applying the rotation matrix to the initial sun vector, and imposing the final sun vector to have a null second component, a positive first one and a negative third component. The result is that the maximum span for the maneuver around X_{sat} is $\pm 90°$.

The maximum time allowed for the maneuver is 360 s. The accuracy required for the manuever is 0.01° along Y_{sat} and Z_{sat}, 0.05° along X_{sat}. For this accuracy it is necessary to consider the flexibility of the arrays. Generally, in fact, the necessity to simulate spacecraft flexibility depends on the level of accuracy required to ACS, because *every spacecraft is flexible to some extent* [6].

2 Dynamics model

A discrete parameters approach has been selected for its better interaction with the Simulink environment. Fig. 2 shows the model of the flexible spacecraft. Each panel is considered as a cantilever beam of length l, with a spring of stiffness K at the root and a mass m at the tip. In this way the first mode of vibration is considered: α represents the angle of deflection of the solar arrays, assumed in opposite verse for each panel.

The analytical mechanics approach has been utilized, finding the equations of motion by means of the Lagrange equations. The Lagrangian problem is formulated in terms of quasi-coordinates [7], thus it takes the form in Eq. (1):

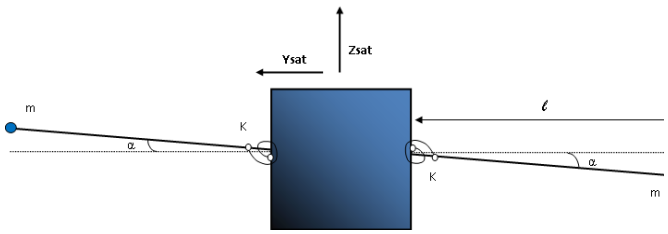

Fig. 2 Solar arrays discrete parameters schematization.

$$\frac{d}{dt}\left(\frac{\partial L}{\partial \omega}\right) + [\tilde{\omega}]\left(\frac{\partial L}{\partial \omega}\right) = Q \qquad (1)$$

L is the Lagrangian function, Q the torque vector, ω the angular rate vector in body coordinates and $\tilde{\omega}$ the skew-symmetric matrix representing the cross product. The equation of the angle α can be expressed by means of the usual Lagrange equation, adding the presence of a dissipation function D, that acts as a natural damping for the system, represented by the Rayleigh damping function [7,8] as in Eq. (2):

$$D = 2\left(\frac{l^2\dot{\alpha}^2}{2}\right)K_d \qquad (2)$$

K_d is the natural damping factor of the system (in kg/s). Thus the equation for the panels deflection can be written as in Eq. (3):

$$\frac{d}{dt}\left(\frac{\partial L}{\partial \dot{\alpha}}\right) - \left(\frac{\partial L}{\partial \alpha}\right) + \left(\frac{\partial D}{\partial \dot{\alpha}}\right) = 0 \qquad (3)$$

The Lagrangian function L is the difference between the kinetic energy and the potential energy, that are expressed in this case as in Eq. (4) [9]:

$$T = \frac{1}{2}\vec{\omega}^T J\vec{\omega} + \sum_{i=1}^{4}\frac{1}{2}I_s{\omega_{ri}}^2 + \sum_{i=1}^{4} I_s\omega_{ri}\vec{\omega}\cdot\hat{a}_i + \frac{1}{2}m\left(\vec{V}_1\cdot\vec{V}_1 + \vec{V}_2\cdot\vec{V}_2\right) + I_p\dot{\gamma}^2 \qquad (4)$$

$$U = \frac{1}{2}K(l^2\alpha^2 + l^2\alpha^2) = Kl^2\alpha^2$$

$\vec{\omega}_{ri}$ represents the i-th wheel angular rate. $\vec{V}_1$ and $\vec{V}_2$ are the linear velocities of the two masses, $J = \begin{bmatrix} A & 0 & 0 \\ 0 & B & 0 \\ 0 & 0 & C \end{bmatrix}$ is the matrix of inertia of the rigid body in body coordinates, not including the presence of the appendages; the body frame is assumed to be the principal frame of inertia, and this implies J to be diagonal. I_p is the beamlike-panel moment of inertia and I_s the wheel polar moment of inertia. $\hat{a}_i$ is the unit vector that expresses the orientation of the i-th wheel axis in the body frame.

In this way it is possible to obtain the equations governing the system: three for the angular rates and one for the deflection. To avoid undesired algebraic loops the system is put in a form as in Eq. (5):

$$T\begin{bmatrix}\dot{p}\\ \dot{q}\\ \dot{r}\end{bmatrix} = -\vec{\omega}\times T\vec{\omega} + U + \tau \qquad (5)$$

where T is the inertia matrix of the entire system, U the control vector and τ the term containing all the coupling terms due to the flexibility. Quaternions kinematics' equations are integrated to compute the spacecraft attitude. The vibration frequency of the panel is evaluated to be 2.2 Hz.

3 Thrusters configuration

The necessity to make maneuvers in relatively short times led to the idea of using reaction thrusters. The selected hardware is an on-off hydrazine-based thruster able to produce 1N thrusts with a rise time of 60 ms, a decay time of 150 ms and a MIB of 2 ms. Thrusters can be accommodated only in the platform module, and in such a way that there is no firing against the payload. The more natural position for thrusters is clearly in the corners of the platform module, so that the arms are maximized, allowing to save fuel. Moreover, if two thrusters are placed in the opposite

direction with respect to the CoM and fired together, the arising torque is independent from the CoM movements due to the reduction of the fuel n the tanks during the spacecraft operative life. An 8 thrusters configuration with a redundancy around *X* has the advantage that it can ensure a higher torque for one and two axes maneuvers, but on the other hand it cannot give a perfect maneuverability for three axes maneuvers. In fact if a thruster gives torques along more than one axis, it is not possible to obtain the desired components of the control torque in body coordinates. Therefore a 12 thrusters configuration has been adopted, as in Fig. 3. This accommodation allows to control the torque along each body axis independently, thus to obtain any of the possible torque components in space.

Once the configuration is chosen, another step can be done in order to minimize the fuel consumption: the thrust directions trade-off. The simple base concept is that the more the thrust direction is tilted with respect to the normal to the satellite, the longer the arm is, with a consequent gain in fuel consumption, until an optimal condition is reached. From the optimal point, continuing inclining the thrust direction would result in a shorter arm, thus in a worst configuration. Obviously the tilt angle shall be the same for each couple of opposite thrusters, to have a null translation when they are actuated. To evaluate the optimal tilt angle, it has been evaluated the torque as function of this angle, as shown in Fig. 4 for *Mx*, the torque around *X*. The curve presents a maximum, corresponding to the optimal tilt angle. The graph is parameterized with respect to the margin to be taken from the satellite borders for thrusters mounting. The analysis demonstrates that considering a margin for the mounting of 20 cm, the optimal tilt angle of the thrusters that provide torques around *X* is 55.9°, while that for thrusters that give torques around *Y* is 49.8°. The thrusters that provide torques around *Z* have been not tilted to avoid plume impingement on the solar arrays.

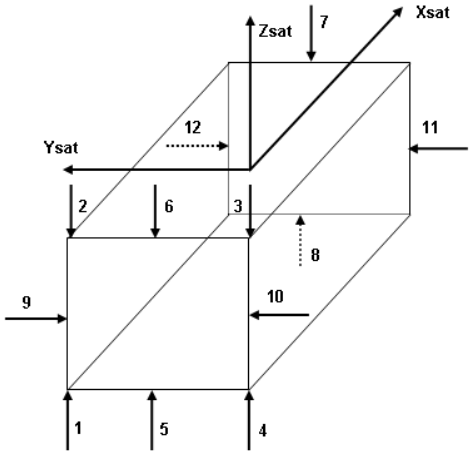

Fig. 3 Thrusters accommodation on the platform module.

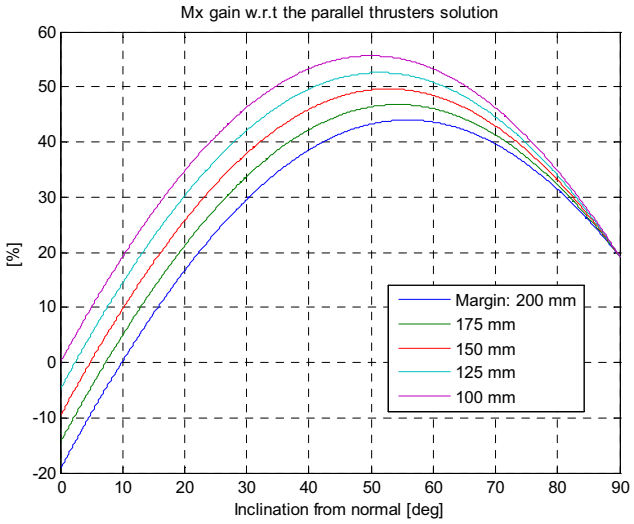

Fig. 4 Mx gain in torque w.r.t the not-inclined thrust directions solution.

4 Control

The complete maneuver has been split into two phases: the *maneuver* and the *fine pointing*. The *maneuver* phase aims to perform the initial part of the maneuver control: its function is to reduce the error between the current attitude and the target attitude beneath a certain threshold. The *fine pointing* phase aims to bring the attitude from the threshold error to the final target, in compliance with the requirements on the accuracy. The schemes for the two phases are shown in Fig. 5. The *maneuver* phase is the part in which the major

effort is required to the ACS hardware, because more than the 95% of the starting attitude error, from the starting condition to the switching condition, is compensated in this phase. In the *fine pointing* phase the attitude error is small: this is a refinement of the maneuver made in the previous phase, and therefore thrusters cannot be useful for intrinsic problems related to their low accuracy. In general, the purely open-loop maneuvers do not require any measurement for feedback, thus there is no possibility of closed-loop instability; nevertheless, in practice, the open-loop schemes are sensitive to the parameters uncertainties and the unexpected disturbances. Therefore a combination of feedforward and feedback control is desirable. For this reason, in the *maneuver* phase thrusters are used in open-loop to provide the change in angular rates needed to perform the maneuver, while reaction wheels are used in closed-loop to compensate disturbances. A slewing guidance gives intermediate targets to the reaction wheels at the controller working frequency. Instead, in the *fine pointing* state a fixed guidance towards the final target is used. An important aspect to consider in the framework of this separation of the controller into two different phases is the criterion to automatically switch from one phase to the other. Different solutions can be taken into account: the chosen one is such that when the *fine pointing* phase is reached, reaction wheels are able to bring attitude within the accuracy in less than 60 s. It is reasonable to admit that the controller can also switch backward, from the *fine pointing* phase to the *maneuver* phase, for example if external disturbances increase the absolute value of the speed and/or the attitude error beyond the limits. Therefore the implementation in the simulator shall grant a two-ways switch.

The chosen control law for the reaction wheels is a PD control known as quaternion feedback [9], and has the form in Eq. (6):

$$\begin{aligned} T_{cx} &= 2K_{p1}q_1q_4 + K_{d1}\omega_1 \\ T_{cy} &= 2K_{p2}q_2q_4 + K_{d2}\omega_2 \\ T_{cz} &= 2K_{p3}q_3q_4 + K_{d3}\omega_3 \end{aligned} \qquad (6)$$

where T_{ci} is the control torque along the i-th body-axis, q_i the components of the error quaternion and ω_i the angular rate error components. K_p and K_d are the proportional and derivative gain matrices. The scalar part of the quaternion, q_4, multiplies the first terms to make the control law robust to its changes in sign, as suggested in [8].

The open-loop control for thrusters is an optimal control that aims to minimize the cost function in Eq. (7).

$$\min J = \int_{t_0}^{t_f} \sum_{i=1}^{3} u_i C u_i^T \, dt + \widetilde{X_f} S \widetilde{X_f}^T \qquad (7)$$

$$subject\ to: \quad \dot{x} = f(x,t) + Bu\,, \quad |u_i| \le 1$$
$$with\ x(t_0) = x_0\ and\ x(t_f) = x_f$$

where $\widetilde{X_f}$ is the error in the final state, t_f is the final time and *C* and *S* the weight matrices. The first term represents the minimization of the propellant consumption, while the second term the minimization of the error on the final state with respect to the target.

However, this solution can be found analytically only for simple problems, for example for the minimum fuel maneuvers of rigid bodies. The dynamics considered in this analysis is strongly non linear for the presence of the solar arrays, and therefore the analytical approach cannot be used. As a consequence, a solution via a numerical approach has been considered. The Matlab function *fmincon* is able to solve the minimization of cost functions in which the states follow a non-linear dynamics, and in presence of constraints.

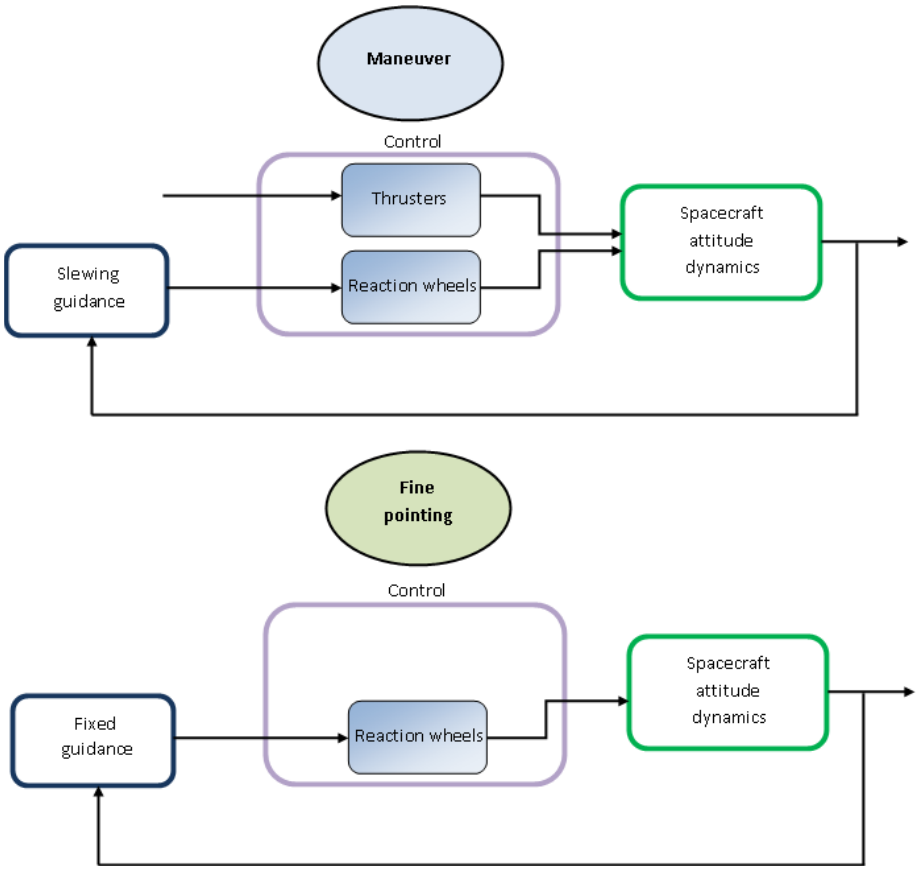

Fig. 5 Control architecture for the two states.

To help the software in solving this not easy problem, two important assumptions have been made:

- the control profile is considered to be piecewise constant: this reduces the number of variables.
- The control profile is considered to be an odd function, that is, anti-symmetric with respect to the half time of the thrusters' firing.

The second assumption is more realistic than it can seem at a first glance: in fact it ensures to have a null angular momentum at the end of the thrusters activation, condition that should be fulfilled by a well-designed maneuver control, while holding the generality of the solution. However these two assumptions surely reduce the search for a minimum to a local optimality problem, that is the found solution will be the best among the possible solutions defined by the two above conditions.
The optimizer software has to work off-line, because the knowledge of the final state is necessary to the computation of the optimal solution. It simulates the dynamics of the spacecraft for the entire time in which thrusters give their contribution. At each step of the optimization process the spacecraft dynamics is simulated, taking into account only the thrusters contribution. Therefore *reaction wheels are not considered in the optimization process*. This ensures that the result is an optimum thrusters contribution, without the help of the wheels. The only simplification made to the simulated dynamics is the *neglecting of the gyroscopic torque*. In a minimum fuel logic, it is reasonable that thrusters have to provide the minimum possible effort, while the reaction wheels have to take care of everything they are able to. In this framework, reaction wheels can therefore compensate for the gyroscopic torque, which is in the order of $1 \cdot 10^{-2}$ Nm, absolutely in the range of the wheels torques. Thus, the slewing guidance of the wheels is based on a dynamics that neglects gyroscopic contribution, and when the real dynamics is simulated, wheels interpret the gyroscopic torque as a disturbance, and act to compensate for it. The compensation is well performed; the error on the final state between a simulation neglecting the gyroscopic torque and a simulation considering it, with the reaction wheels in the control loop, is in the order of $1 \cdot 10^{-2^\circ}$ in eigen-angle.

A Pulse Width Modulation (PWM) technique is used to modulate the thrust of the on-off thrusters. Also this effect is neglected in the optimization process, where adjustable torques are considered as provided from the thrusters. As for the gyroscopic torque, the PWM effect is compensated by reaction wheels in the real dynamics simulation. This avoids numerical problems created by the presence of the PWM in the optimization process.

In the minimum fuel consumption problem, the spacecraft dynamics is simulated at each step of the optimization process. Thus the state profile during the entire firing time interval using the optimal control is known at the end of the process. This profile represents the state trajectory if only thrusters are used, and therefore it can be used as a slewing guidance for the reaction wheels in the simulation of the "real" dynamics.

5 Simulations and results

The model of the flexible attitude dynamics described in section 2 has been implemented in Matlab Simulink environment. The model has been tested to verify its correct functioning. Several characteristic cases have been performed: rigid body, harmonic oscillator, spinning body, body at rest with oscillating panels, etc… The results of the simulations are identical to the expected behavior in all the cases. Therefore the model is considered validated. Details of the test campaign are in [10].

A comparison of the model with a simple one representing the attitude dynamics of a rigid body demonstrates that the difference is not negligible during the fine pointing phase, as it is shown in Fig. 6. The simulation starts from initial conditions for attitude and speed of switch to the *fine pointing* phase, and initial deflection of the arrays of 0.05°. The system is forced to reach zero by the reaction wheels. It is to notice that the difference between the attitude of the two models, expressed in eigen-angle, is more than 10 times the required accuracy of 36 arcsec during fine pointing.

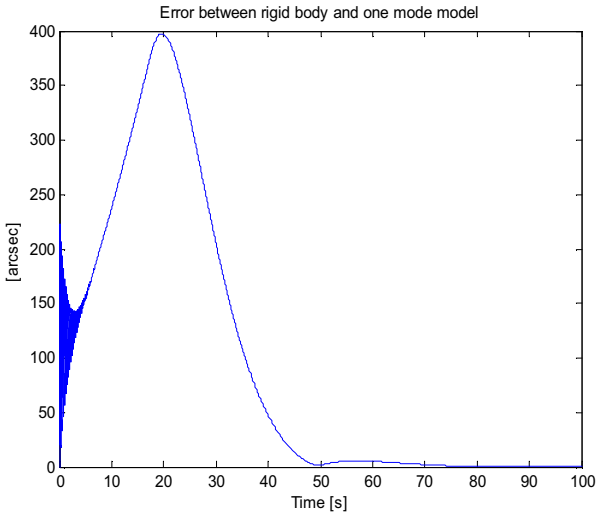

Fig. 6 Difference in eigen-angle between the rigid body and the flexible body models, in arcsec.

One axis maneuvers are examined first. The worst-case maneuver of this kind is a 90° rotation around *X*. The control profile obtained from the optimization process is shown in Fig. 7. Thrusters fire for the first 200 s. Defining the fuel consumption as the integral over time of the sum of the modules of the control variables (being *u* dimensionless the result is in seconds), the consumption for this control profile is 30.1 s, which corresponds to a hydrazine consumption of 40 grams considering a specific impulse of 150 s. The control profile obtained from the optimization process has been used then for the simulation of the entire maneuver, resulting in the states profiles shown in Fig. 8 and Fig. 9. 8° from the final target are reached in the first 200 s: as expected, reaction wheels have perfectly compensated for gyroscopic torque and PWM effects. After the thrusters contribution, the *maneuver* phase is completed by the reaction wheels, until the switch conditions are reached and the *fine pointing* phase is performed. The maneuver reachesa the final target within the accuracy nd widely within the required time, as shown in Fig. 10.

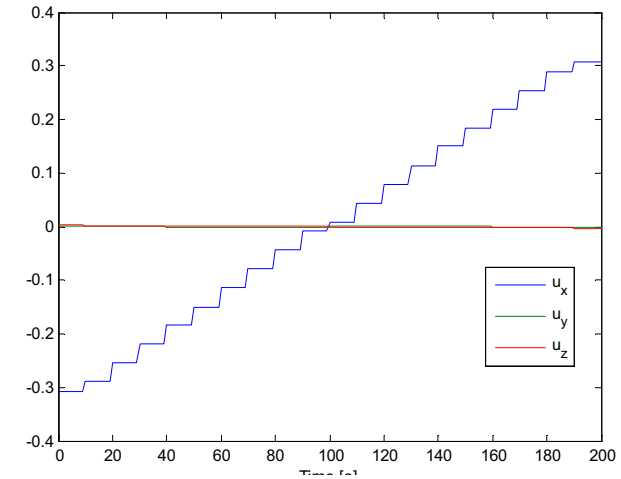

Fig. 7 Control profiles for a (90°,0,0) maneuver.

The array deflection is reported in Fig. 11. It is clear that the frequent burns due to the Pulse Width Modulation excite continuously the panels, resulting in wide oscillations for the first 200 s. While thrusters are firing in the first 200 s, wheels have to compensate for gyroscopic torque and PWM effects. The maximum speed peak reached by the wheels is of 2500 rpm, which is in the acceptable range for the selected hardware.

Results for the other one axis maneuvers are analogous, with a saving in time in the order of 50-60 s with respect to the maximum allowed time for reaching the desired accuracies, and with a consumption of no more than 35 s.

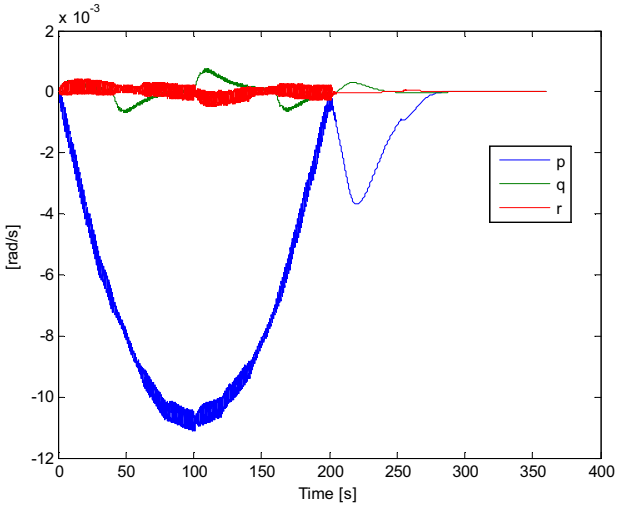

Fig. 8 Angular rates profiles for a (90°,0,0) maneuver.

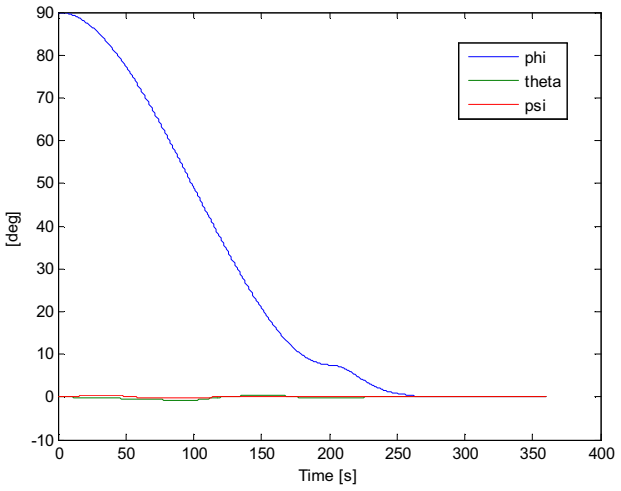

Fig. 9 Attitude profiles for a (90°,0,0) maneuver.

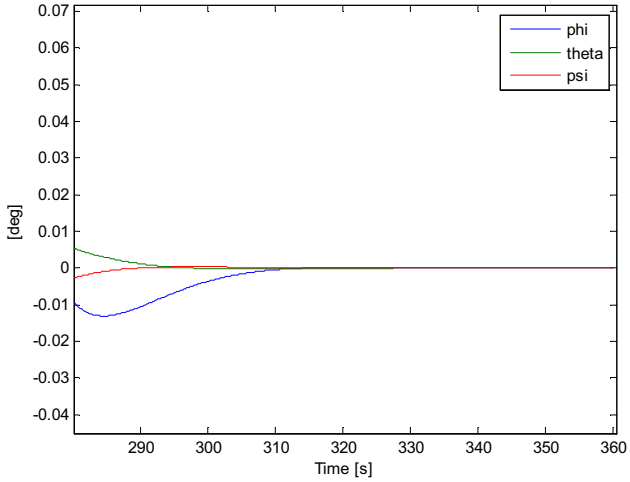

Fig. 10 Accuracy is reached in less than 290 s.

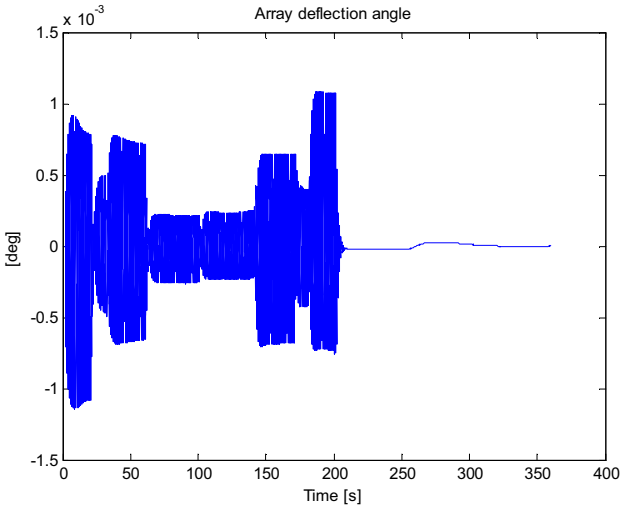

Fig. 11 Array deflection angle during maneuver.

The worst-case for three axes maneuvers is a (-90°,45°,45°) slew. In this case the control profile obtained from the optimization process is that in Fig. 12. This control ensures a consumption of 51.4 s, 69 g of hydrazine. The attitude profile obtained for the entire maneuver is depicted in Fig. 13.
The maneuver is correctly performed: the attitude reaches the target in the fixed time within the required accuracy. The accuracy range is reached 40 s before the fixed final time.

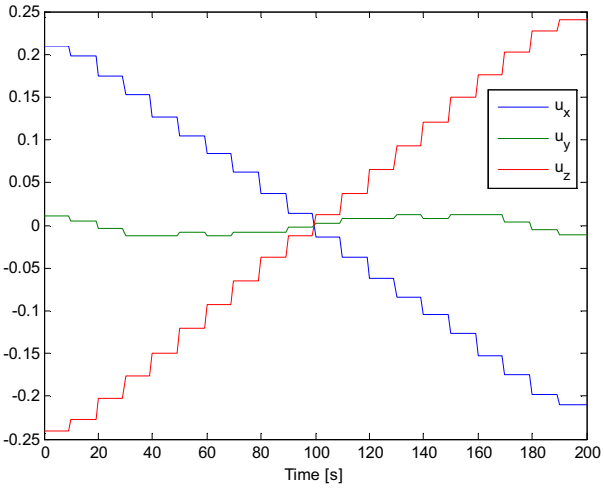

Fig. 12 Control profiles for a (-90°,45°,45°) maneuver.

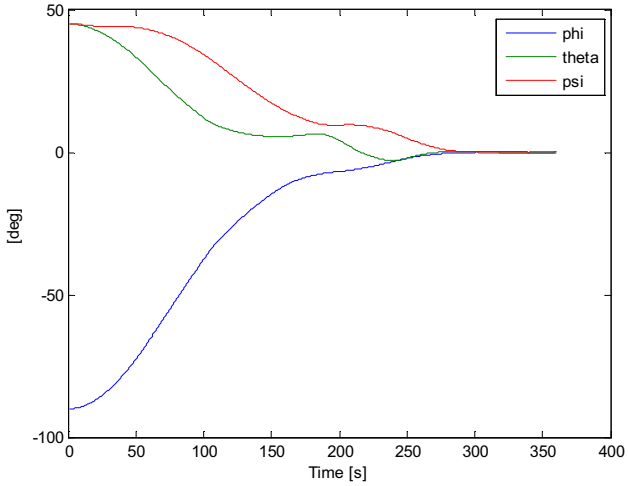

Fig. 13 Attitude profiles for a (-90°,45°,45°) maneuver.

Table 2 summarizes the obtained results, giving evidence of the behavior of the developed control strategy with the maneuver requirements.

Table 2 Results obtained with the developed control strategy.

ONE AXIS MANEUVERS	
Error after 360 s	$1 \cdot 10^{-5}$°
Time to reach the accuracy range	290-328 s
Fuel consumption	30.1-35.2 s
THREE AXES MANEUVERS	
Error after 360 s	$1 \cdot 10^{-4}$°
Time to reach the accuracy range	320 s
Fuel consumption	51.4 s

6 Conclusion

The analytical model of the flexible dynamics has been developed, implemented and fully validated. Thrusters have been accommodated on board the platform module in order to reduce fuel consumption, ensuring at the same time sufficient thrusts for the maneuvers. Thrust directions have been tilted with respect to the satellite faces in order to increase the available torques, and optimal tilt angles have been found numerically.
The control strategy has been developed to obtain a minimum energy-minimum error strategy, that is a control that brings the attitude close to the target, saving the maximum possible amount of fuel. Since the problem was not solvable analytically, a numerical approach has been used. An optimizer algorithm has been developed using the Matlab function *fmincon*. At the end of the optimization process the optimum control profile is obtained and utilized for a simulation of the entire maneuver. Tests demonstrate that the considered control strategy allows performing the worst-case maneuvers, ensuring to reach the final target within the required accuracy and time. After 360 s, the maximum allowed time for the maneuver, the attitude error with respect to the target is always below $1 \cdot 10^{-4}$°, that is two

orders of magnitudes less with respect to the required accuracy. The range of admissible error – the accuracy range – is always reached in 320-330 s, saving 40 s w.r.t the maximum allowed time in the worst-case three axes maneuver, and even 70 s for the worst-case one axis maneuver around X_{sat}. Propellant consumption is far inferior to that of a not-optimal maneuver.

References

[1] Vadali S.R., Carter M.T., Singh T., Abhyankar N.S., "Near-minimum-time maneuvers of large structures: theory and experiments", *Journal of Guidance, Control and Dynamics*, Vol. 18, No. 6, 1995.

[2] Hall C.D., Tsiotras P., Shen H., "Tracking rigid body motion using thrusters and reaction wheels", AIAA 98-4471.

[3] Singh G., Kabamba P.T., McClamroch N.H., "Planar, time-opimal, rest-to-rest slewing maneuvers of flexible spacecraft", *Journal of Guidance*, Vol. 12, No. 1, 1989.

[4] Ebrahimi A., Moosavian S.A.A., Mirshams M., "Control of space platforms with flexible links using command shaping method", *Iranian Journal of Science & Technology*, Vol. 32, No. B1, 2008.

[5] Anthony T.C., Wie B., Carroll S., "Pulse-modulated control synthesis for a flexible spacercaft", *Journal of Guidance,* Vol. 13, No. 6, 1990.

[6] Wertz J.R., *Spacecraft Attitude Determination and Control*, Kluwer Academic Publishers, 1978.

[7] Meirovitch L., *Methods of analytical dynamics*, McGraw-Hill.

[8] Sidi M.J., *Spacecraft dynamics and control. A practical engineering approach,* Cambridge University Press, 1997.

[9] Wie B., Barba P.M., "Quaternion feedback for spacecraft large angle maneuvers", *Journal of Guidance,* Vol. 8, No. 3, 1985.

[10] Paolini E., "Large attitude maneuvers of a spacecraft with flexible appendages", Master Degree Dissertation in Astronautical Engineering, School of Aerospace Engineering, University of Rome La Sapienza, Italy, 2011.